Adsorption 11: 15–29, 2005

Empirical Multicomponent Equilibrium and Film-Pore Model for the Sorption of Copper, Cadmium and Zinc onto Bone Char

CHUN-WAI CHEUNG, KEITH K.H. CHOY, JOHN F. PORTER AND GORDON MCKAY*
Department of Chemical Engineering, Hong Kong University of Science and Technology, Clear Water Bay Road, Kowloon, Hong Kong SAR, China
kemckayg@ust.hk

Received June 30, 2003; Revised September 14, 2004; Accepted November 3, 2004

Abstract. The adsorption of three metal ions onto bone char has been studied in both equilibrium and kinetic systems. An empirical Langmuir-type equation has been proposed to correlate the experimental equilibrium data for multicomponent systems. The sorption equilibrium of three metal ions, namely, cadmium (II) ion, zinc (II) ion and copper (II) ion in the three binary and one ternary systems is well correlated by the Langmuir-type equation. For the batch kinetic studies, a multicomponent film-pore diffusion model was developed by incorporating this empirical Langmuir-type equation into a single component film-pore diffusion model and was used to correlate the multicomponent batch kinetic data. The multicomponent film-pore diffusion model shows some deviation from the experimental data for the sorption of cadmium ions in Cd-Cu, Cd-Zn and Cd-Cu-Zn systems. However, overall this model gives a good correlation of the experimental data for three binary and one ternary systems.

Keywords: film-pore diffusion, batch sorption, metal ions, bone char, multicomponent

Introduction

Sorbent performance is the critical factor in the design and operation of an adsorption system. Bone char is a heterogeneous sorbent which is derived from the calcination of animal bone in the absence of air. This sorbent has been demonstrated to remove aluminum ions and iron ions from rural water in a pilot study (Lewis, 1995). Therefore, it is believed that bone char can be used to remove metal ions from wastewaters.

Bone char, a mixed adsorbent containing around 10% carbon and 90% calcium phosphate, is mainly produced by the carbonization of bones. Structurally, the calcium phosphate in bone char is in the hydroxyapatite form Girgis et al. (1997). It has been shown that after the decarbonization of bone char it has little or no decolorizing power (Elliott, 1994), although the hydroxyapatite in bone char retains an adsorption capacity to adsorb calcium salts (Killedar, 1991) and dissolved salts (Elliott, 1994). Therefore, bone char can eliminate either organic or inorganic species from their solutions.

Bone char has traditionally been used to decolourize sugar solutions in the sugar refining industry for many years. Abdel Raouf and Daifullah (1997) reported that the bone char derived by heating the animal bone to 500–600°C could be used to remove fluoride from drinking water on a laboratory scale (Christoffersen et al., 1991; Larsen et al., 1993; Phantumvanit and LeGeros, 1997). In recent studies, bone char was used to adsorb the radioisotopes of antimony and europium ions from radioactive wastes (Bennett and Abram, 1967). The authors suggested that chemisorption was the main operating mechanism for $^{152}Eu^{3+}$ removal with a high degree of irreversibility fixation on bone charcoal from the aqueous solution. The authors claimed the sorption was due to the cation exchange of metal ions onto hydroxyapatite. In contrast, physical

*To whom correspondence should be addressed.

Table 1. Physical and chemical properties of bone char.

Chemical composites		Physical properties	
Items	Limits	Items	Limits
Acid insoluble ash	3 wt.% max.	Bulk density (Dry)	640 kg/m^3
Calcium carbonate	7–9 wt.%	Carbon surface area	50 m^2/g
Calcium sulfate	0.1–0.2 wt.%	Moisture	5 wt.% max.
Carbon content	9–11 wt.%	Pore size distribution	7.5–60,000 nm
Calcium HAP	70–76 wt.%	Pore volume	0.23 cm^3/g
Iron-as Fe_2O_3	<0.3 wt.%	Total surface area	100 m^2/g

Source: Tate & Lyle Company Limited.

sorption was suggested to be the main mechanism to remove radioactive organic solutions of antimony when loaded from the liquid organic radioactive wastes. Gu and coworkers (Gu et al., 1998) found that both bone char and iron impregnated bone char could remove the uranyl ions (UO_2^{2+}) from wastewater.

As studies into the sorption of metal ions onto bone char are relatively limited in number, studying the sorption of metal ions onto pure hydroxyapatite may assist in indetifying the sorption properties of metal ions onto bone char. Suzuki and coworkers (Suzuki et al., 1982, 1985, 1991) have studied the sorption capacity of metal ions onto CaHAP. In recent work, Suzuki and coworkers (Hatsushika et al., 1999) concluded that the order of cation sorption according to the amount of exchange by the original CaHAP is as follows:

$$Fe^{2+} \gg Pb^{2+} > Cr^{3+} > Y^{3+} \geq La^{3+} > Al^{3+} > Cu^{2+} > Zn^{2+} > Mn^{2+} > Ni^{2+} > Cd^{2+} = Co^{2+}$$

In the present work, bone char has been used to remove copper, cadmium, and zinc from aqueous effluent in three binary and one ternary agitated batch-contact systems. Equilibrium capacities were determined and analysed and a multicomponent mass transport model, based on film pore diffusion and incorporating an empirical equilibrium model, has been developed and tested.

Experimental Materials and Procedures

Bone Char

The bone char used in this study was Brimac 216, 20/60 mesh supplied by Tate & Lyle Process Technology. The physical and chemical properties of bone char were analyzed by the manufacturer. Table 1 shows that the main composition of bone char is calcium hydroxyapatite. The chemical formula of calcium hydroxyapatite is $Ca_{10}(PO_4)_6(OH)_2$ or $Ca_5(PO_4)_3(OH)$ and Fig. 1 shows the structure of CaHAP. The carbon is distributed throughout a porous structure of hydroxyapatite in the bone char. The manufacturer used the adsorption of cetyltrimethylammonium bromide (CTAB) from water to measure the carbon surface area and the adsorption of sodium di-2-ethylhexyl sulfosuccinate (Manoxol OT) from water to measure the total surface area (Bennett and Abram, 1967). Although the manufacturer did not use the B.E.T isotherm to measure the surface area of the bone char, the B.E.T isotherm was used to measure the pore volume distribution in this research. The BET surface area of the bone char was determined using an Omnisorp Coulter 100CX unit and the BET surface

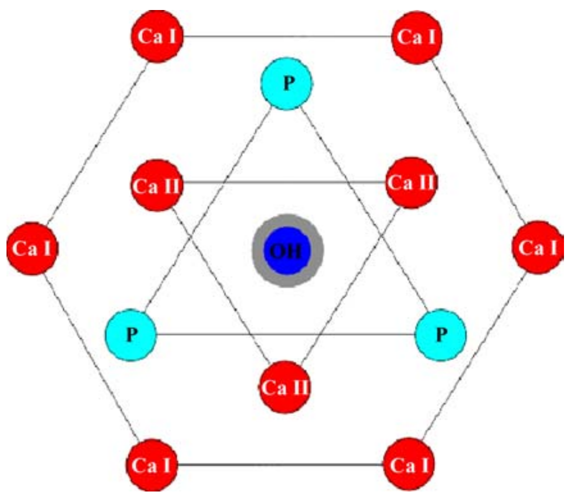

Figure 1. The structure of calcium hydroxyapatite.

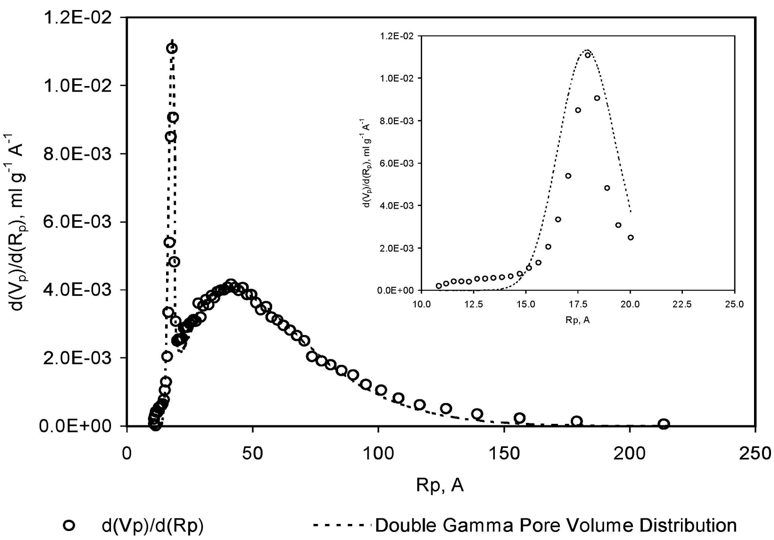

Figure 2. The Pore volume distribution of bone char using N_2 condensation and evaporation.

area of bone char was measured as 130 m^2/g. Figure 2 shows the pore volume distribution against the pore size of bone char. The pore volume distributions against pore size are separated into two regions. The mean pore diameters after unit conversions are equal to 3.6 and 11.2 nm. According to the classification of pore size as recommended by IUPAC (Do, 1998), these are mesopores (2 nm $< d_{\text{pore}} <$ 50 nm). As a hydrated metal ion is relatively small relative to the average pore diameter, it can freely diffuse along the pore to the center of sorbent. Hence, pore diffusion has been considered as a main rate-controlling mechanism in these present studies.

Pretreatment of Bone Char

The bone char was sieved to separate the material into discrete size ranges. In this research, the adsorption properties of 500–710 μm particle size bone char were studied. After sieving the char, the adsorbent was rinsed with deionized water. Finally, the adsorbents were dried at 103–105°C for 24 hours, and then allowed to cool in the dessicator. The pH value of 1 g of bone char in 1 l of deionized water is 9.

Sorbate

Sulfuric acid is a commonly used acid in industry; therefore, the wastewater usually contains sulfate ions in solution. In this research, analytical grade cadmium (II) sulfate ($3CdSO_4{\cdot}8H_2O$) and copper (II) sulfate ($CuSO_4{\cdot}5H_2O$) used in the experiments were supplied by Riedel-de Haën Chemicals. The analytical grade zinc (II) sulfate ($ZnSO_4{\cdot}7H_2O$) was supplied by BDH chemicals. Stock solutions of metal ions were prepared using deionized water. All solutions were adjusted to $\text{pH} = 4.9 \pm 0.1$ using dilute sulfuric acid. If metal chloride or metal nitrate is used, the sorption capacity and sorption rate of metal ions onto bone char may be different (Suzuki et al., 1985).

Analytical Techniques

The concentrations of metal ion solutions were measured by Inductively Coupled Plasma-Atomic Emission Spectrophotometer (ICP-AES). The samples were diluted five times by deionzied water; therefore, the concentrations of the metal ion solutions should be in the range of 0 to 90 mg/dm^3. The calibration standards were prepared using the standard solutions and five calibration standards (5, 15, 30, 60 and 90 mg/dm^3) were prepared for calibrating the machine before measuring. A linear calibration line (correlation coefficient $R^2 > 0.999$) was obtained after calibration to ensure the accuracy of results. The samples were automatically measured three times in one aspiration. If the difference of three test results was greater than one percent, the samples were measured again until the test results fulfilled the analysis requirement.

Equilibrium Contact Time

When the agitation time required for the equilibrium sorption isotherm is determined, the experimental sorption equilibrium isotherms for single and multicomponent systems will be determined according to this limiting contact time. The sorption of metal ions from solution took 72 hours to reach equilibrium for all three metal ions. To ensure equilibrium was attained, agitation was performed for five days for all equilibrium experiments.

Sorption Equilibrium Isotherm

A fixed mass, 0.25 g, of bone charcoal was weighed into 120 ml test bottles. Metal ion solutions were prepared and then 50 ml was pipetted into each test bottle. The initial pH of the solutions was adjusted to 4.9 ± 0.1 by the addition of dilute sulfuric acid. The test bottles were put in the shaker bath for five days and were shaken at the maximum shaking rate (200 rpm) to allow the bone charcoal to adsorb the metal ions until the solution reached equilibrium. The initial and final concentrations of the solutions were measured by ICP-AES. These data were used to calculate the adsorption capacity, q_e, of the adsorbent. Finally, a diagram of adsorption capacity, q_e, against equilibrium concentration, C_e, was plotted. The amount of metal ion sorbed, q_e, was calculated from:

$$q_e = \frac{(C_o - C_e)V}{W} \tag{1}$$

In the batch kinetic study, the sorption capacity at time t, q_t, was calculated by replacing C_e with C_t in Eq. (1).

Batch Kinetic Mass Transport Studies

These experiments were used to study the influence of sorbent mass and initial metal ion concentration on the adsorption rate. An adsorber vessel in a standard batch stirred-tank configuration was used in all of the experiments. A standard tank configuration was used to derive the relative dimensions of the vessel and its components (Furusawa and Smith, 1973). The following relationships hold with respect to the vessel inside diameter, D_i (see Fig. 3).

Height of baffles = 0.2 m
Baffle width = 0.075 D_i

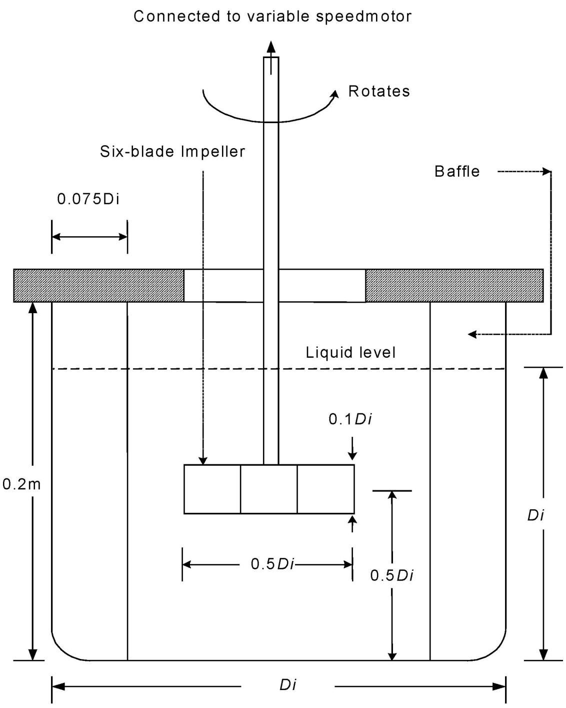

Figure 3. Standard tank configuration for contact time studies.

Height of liquid in the vessel = D_i
Distance between impeller blade and vessel bottom = 0.5 D_i
Height of impeller blade = 0.1 D_i
Impeller diameter = 0.5 D_i

The adsorber vessel was a 2 dm^3 plastic beaker with 0.13 m internal diameter and it can hold a volume of 1.70 dm^3 acid dye solution for the batch contact time experiment. A six bladed, flat plastic impeller was used to enhance mixing. The diameter of the impeller and the blade height were 0.065 m and 0.013 m respectively. A Heidolph variable motor was used to drive the impeller using a 0.005 m diameter plastic shaft. Six plastic baffles were evenly spaced around the circumference of the vessel, positioned at 60° intervals and held securely in place on top of the vessel. Polystyrene baffles were 0.2 m long and 0.01 m wide. The purpose of the baffles were used to prevent the formation of a vortex, to reduce the relative motion between liquid and solid particles consequentially, and to reduce power losses due to air entrainment at the impeller. They were secured in a position slightly away from the vessel wall and bottom of the tank in order to prevent particle accumulation. Evaporation of liquid was prevented by using a thick polystyrene sheet on top of the vessel.

Table 2. The effect of the concentration and mass.

Concentration (mM)	Mass (g)
2	6.5
2.5	7.5
3	8.5
4	9.5
5	10.5

Note: Temperature = 20°C, pH = 4.9, Particle size = 500–710 μm.

The standard condition was fixed at the mass of bone char (8.5 g), at a fixed particle size (500–710 μm), a fixed temperature (20 ± 2°C), a fixed pH (4.90 ± 0.10), and a fixed initial concentration of metal ion solution 3 mM (see Table 2). Therefore, the effect of initial concentration of metal ion solution on the adsorption rate was studied by varying the initial concentrations of metal ion solution (i.e. 2, 2.5, 3, 4 and 5 mM) and the other conditions were fixed. The effect of sorbent mass was studied using the same conditions as defined in standard conditions. Several experiments were repeated to ensure that the experimental values are reproducible.

In the batch kinetic study, the effect of the initial concentrations and the volume to mass ratios for the adsorption isotherms were investigated. The operating lines of Cd ions for different systems are presented in Fig. 4. Figure 4 shows that the equilibrium capacities, q_e, change at different initial concentrations and volume to mass ratios, V/M. The kinetic data started at an initial concentration, C_o at $t = 0$, and the operating lines can then be plotted terminating on the sorption isotherm, C_e at $t = \infty$. The operating lines for the variation of adsorbate concentration (solid lines) and adsorbent mass (dashed lines), see Table 2, in batch kinetic studies almost covers the whole region of adsorption isotherm.

Theory of Film-Pore Diffusion Model

A previous paper (Cheung et al., 2001) introduced the use of an analytical method to determine the external mass transfer coefficients and the pore diffusion coefficients. The analytical method can provide a good correlation of experimental data when all operating lines terminate on the saturation region of the equilibrium isotherm curve (i.e. $q_{e,t} = q_{e,h} = q_m$). However, when the operating lines do not terminate on the saturation region of the equilibrium isotherm curve, the hypothetical equilibrium concentration must be assumed to be a certain value before calculation. In order to calculate the effective diffusivity accurately in the present work, the hypothetical equilibrium concentration, $q_{e,h}$,

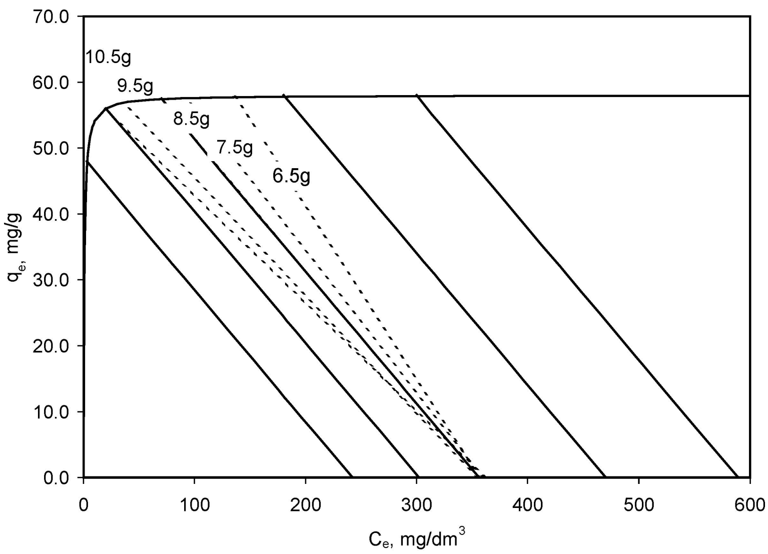

Solid lines – operating lines for variation of adsorbate concentration

Dashed lines – operating lines for variation of adsorbent mass

Figure 4. The relationship of adsorption isotherm and the mass transport model. (Operating line plots for Cd ions systems).

is replaced by the solid phase concentration, $q_{e,t}$. Since $q_{e,t}$ is a variable in the equation, the film-pore diffusion model must be solved by a numerical method. The theoretical assumptions of this numerical film-pore diffusion model are:

(1) The adsorbate is transferred within the pores of the bone char particle solely by means of molecular diffusion.
(2) Adsorption equilibrium according to the isotherm is presumed between the pore-water and the bone char throughout. In other words, the deposition-rate of the metal ions in the pore water onto the bone char surface is taken to be much higher than their rate of diffusion.
(3) The solid-phase concentration at the bone char surface, $q_{e,t}$, is a function of liquid-phase concentration on the bone char surface, $C_{e,t}$.
(4) The quantity of adsorbate in the pore water is much lower than that on the bone char per unit volume and can therefore be neglected.

Calculation of Adsorption Rate

This model is based on the unreacted shrinking core pore diffusion model and the main equations of this model are summarized here as the derivation has been presented previously (Cheung et al., 2001). The external mass transfer rate at the external surface of the bone char particles is given by:

$$N_t = k_f 4\pi R^2 (C_t - C_{e,t}) \tag{2}$$

According to the first Fick's law, the pore diffusion rate in the pore water is:

$$N_t = \frac{4\pi D_{\mathrm{eff}} C_{e,t}}{1/r - 1/R} \tag{3}$$

The velocity of the concentration front is given by:

$$N_t = -4\pi r^2 q_{e,t} \rho_p \frac{\mathrm{d}r}{\mathrm{d}t} \tag{4}$$

The average concentration in the sorbent is given by:

$$q_t = q_{e,t}\left[1 - \left(\frac{r}{R}\right)^3\right] \tag{5}$$

The mass balance of the sorbent is given by:

$$q_t = (C_o - C_t)\frac{V}{W} \tag{6}$$

Numerical Solution for Concentration Decay Curve

The mass transfer from the bulk solution across the liquid film is equal to intraparticle diffusion of sorbate. Therefore, combining Eqs. (2) and (3) gives the relationship between the concentration of sorbate in bulk solution and the concentration on the sorbent surface:

$$C_t = \left[1 + \frac{D_{\mathrm{eff}} r}{k_f R(R-r)}\right] C_{e,t} \quad \text{or} \quad C_t = \psi C_{e,t} \tag{7}$$

The mass balance of solid phase and liquid phase from Eqs. (5), (6) and (7) becomes:

$$W\left[q_{e,t}\left(1 - \left(\frac{r}{R}\right)^3\right)\right] = V(C_o - \psi C_{e,t}) \tag{8}$$

The concentration of sorbate on the surface at radius r is equal to $C_{e,t}$. The Langmuir equation is used to relate equilibrium concentrations on the solid phase surface. Therefore, the solid phase concentration at r can be represented by:

$$\text{Langmuir equation:} \quad q_{e,t} = \frac{q_m a_L C_{e,t}}{1 + a_L C_{e,t}} \quad \text{or} \quad q_{e,t} = \frac{K_L C_{e,t}}{1 + a_L C_{e,t}} \tag{9}$$

Due to the complex nature of the metal ion sorption process involving exchange sorption and active carbon sorption on the surface, several isotherm models were tested to correlate the experimental data. Despite, at least a dual sorption reaction step being involved, on this heterogeneous surface the Langmuir equilibrium isotherm model equation provided an excellent correlation with the single component experimental data. The excellent fits can be seen qualitatively in Figs. 5 and 6. Furthermore, a significant monolayer effect can be seen for all the single component systems, which is also characteristic of Langmuir monlayer equilibrium saturation. There is no steady rise in the solid phase sorption capacity as observed in an isotherm curve characteristic of the Freundlich isotherm and typifying heterogeneous adsorption systems. Consequently, in the present work a Langmuir type mathematical relationship has been used to describe the three metal

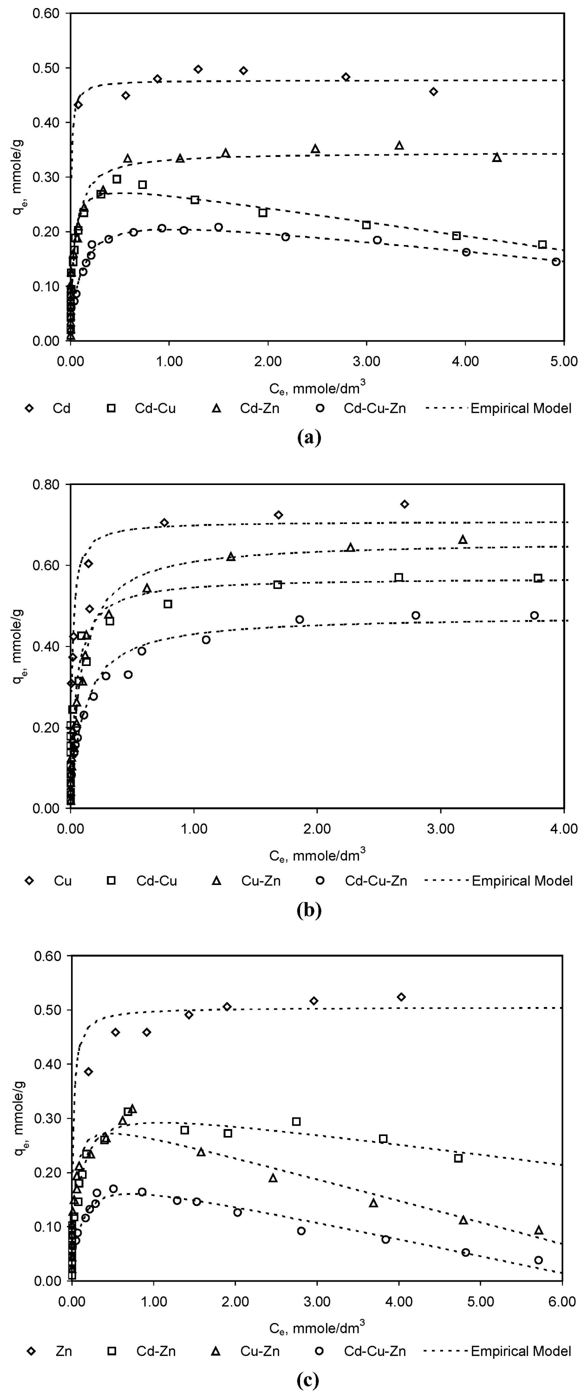

Figure 5. Sorption of Cd (a), Cu (b) and Zn (c) ions onto bone char from single and multicomponent systems (Temperature = 20°C, pH = 4.9, Particle Size = 500–710 μm).

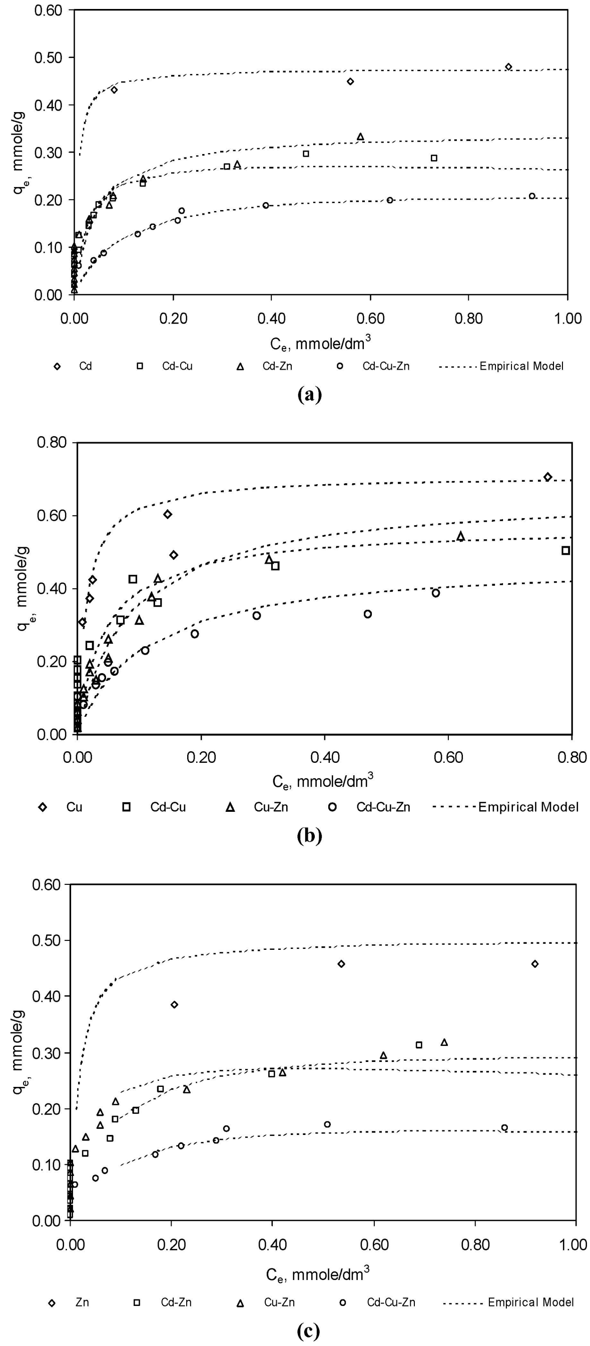

Figure 6. Sorption of Cd (a), Cu (b) and Zn (c) ions onto bone char from single and multicomponent systems (Temperature = 20°C, pH = 4.9, Particle Size = 500–710 μm).

ions—bone char adsorption systems. The quality of the fit of the Langmuir type equation is probably due to the fact that the sorption activation energies are both low and of a similar order magnitude.

In the previous model (Cheung et al., 2001), a rapid analytical solution has been developed by assuming $q_{e,t}$ is a constant value equal to $q_{e,h}$. In this model, the tie lines and time-dependent values for $C_{e,t}$ and, hence, $q_{e,t}$ can be obtained. Combining Eqs. (8) and (9) and letting $R_m = (1 - (r/R)^3)(W/V)$, the following quadratic equation is obtained:

$$a_L \psi C_{e,t}^2 + (\psi + a_L q_m R_m - a_L C_o) C_{e,t} - C_o = 0 \tag{10}$$

From the quadratic Eq. (10), $C_{e,t}$ can then be solved in terms of the shrinking radius (Cheung et al., 2001).

$$C_{e,t}(r) = \frac{-(\psi + a_L q_m R_m - a_L C_o) + \sqrt{(\psi + a_L q_m R_m - a_L C_o)^2 + 4 a_L \psi C_o}}{2 a_L \psi} \tag{11}$$

The intraparticle diffusion of sorbate is equal to the velocity of the concentration front. Therefore, combining Eqs. (3), (4) and (9), the rate equation becomes:

$$\frac{\Delta r}{\Delta t} \cong \frac{\mathrm{d}r}{\mathrm{d}t} = -\frac{D_{\text{eff}}(1 + a_L C_{e,t})R}{q_m a_L r (R - r)\rho_p} \tag{12}$$

or

$$\Delta r = -\left(\frac{D_{\text{eff}}(1 + a_L C_{e,t})R}{q_m a_L r (R - r)\rho_p}\right)\Delta t \tag{13}$$

Since $C_{e,t}$ is known as a function of r, Eqs. (7), (11) and (13) can be solved for a specified time by a numerical method. The solution scheme proposes that the shrinking core radius can be calculated by Eq. (14).

$$r^{j+1} = r^j + \Delta r^j \tag{14}$$

The shrinking core radius at $t = 0$, r^0, is assumed to be the arithmetic mean radius between respective mesh sizes of the sorbent ($r^0 = d_p/2 = 3.03 \times 10^{-2}$ cm). The initial guess of the time interval ($t = 0$), Δr^0 in the numerical program are 0.2 s and -1×10^{-5} cm. Therefore, at time equal to t^1, the shrinking core radius, r^1, the deta radius, Δr^1, and the concentration of solution on the surface at time t^1, $(C_{e,t})^1$, can be calculated using Eqs. (11) and (13), respectively. Therefore, Δr^j can be calculated from $(C_{e,t})^j$. The concentration of solution on the surface at time t can be obtained by repeating the calculation of $(C_{e,t})^j$ and r^j. Since the concentration of solution on the surface cannot be measured, Eq. (7) will be used to calculate the sorbate concentration in solution. The adjustable parameters in Eqs. (7), (11) and (13) are the film diffusion coefficient, k_f, and effective diffusivity, D_{eff}. Therefore, the constants k_f and D_{eff} can be found by minimizing the Sum of Square of Errors, *SSE*, between the experimental and the theoretical concentration for experimental C_t values.

$$SSE_{\text{total}} = \sum_{j=1}^{n} \left\{ \sum_{i=1}^{m} [(C_t)_{\text{exp},i} - (C_t)_{\text{calc},i}]^2 \right\}_j \tag{15}$$

Mass Transport for the Multicomponent Systems

This film-pore diffusion model can be used to correlate the experimental data for multicomponent systems if the diffusion (film and pore) process of each adsorbate onto the adsorbent is independent of the other adsorbates and behaves the same as the single component diffusion process. Therefore, the diffusion equations for each component can be solved independently and the sorption kinetics for the multicomponent systems can be treated as a single component. The calculation of adsorption equations used in this part is similar to that for a single component system. However, the Langmuir equation fails to correlate the adsorption isotherms for the sorption of cadmium and zinc ions with copper ions in the multicomponent system because the sorption of cadmiun and zinc ions onto bone char is negatively impacted by copper ions at high concentration systems. Hence, an empirical equation is derived and used when the Langmuir equation is not fitted. The starting point of this numerical method is the assumption that the mass transport rate of metal ions from the bulk solution across the liquid film is equal to the diffusion rate of metal ions to the interior of the particle.

An empirical Langmuir-type equation is used to describe the time-dependent surface or tie-line concentration at time t on the sorbent surface as derived below in Eq. (16). It is proposed that the sorption of one of the metal ions on the solid phase can be correlated by the Langmuir equation. However, parts of the sorption component of the metal ions, which can be correlated by the Henry's law, are displaced by the copper ions. The Henry equation solid phase displacement subtracted from the Langmuir equation becomes the solid phase concentration for the other metal ions, as defined by Eq. (16):

$$q_{e,t} = \frac{q_m a_L C_{e,t}}{1 + a_L C_{e,t}} - H C_{e,t} \quad (16)$$

Combining Eqs. (8) and (16) and substituting $R_m = (1 - (r/R)^3)(W/V)$ yields the quadratic equation:

$$a_L(\psi - H R_m)C_{e,t}^2 - (a_L C_o - (\psi + R_m(q_m a_L - H)))C_{e,t} - C_o = 0 \quad (17)$$

From the quadratic Eq. (17), $C_{e,t}$ can then be solved as a function of the shrinking core radius.

$$C_{e,t}(r) = \frac{(a_L C_o - (\psi + R_m(q_m a_L - H))) + \sqrt{Dis}}{2a_L(\psi - HR_m)} \quad (18)$$

where

$$Dis = (a_L C_o - (\psi + R_m(q_m a_L - H)))^2 + 4a_L C_o(\psi - HR_m) \quad (19)$$

Therefore, the equilibrium concentration on solid surface is a function of the shrinking core radius. Since $C_{e,t}$ is known as a function of r, Eqs. (7), (13) and (18) can be solved for a specified time by a numerical method. The solution scheme proposes that the shrinking core radius can be calculated by Eq. (14). The above numerical scheme can be used to estimate values of the pore diffusivities for the sorption of three binary metal ions for the multicomponent systems.

Results and Discussion

In our previous studies (Cheung et al., 2001), we successfully demonstrated the ability of the film-pore diffusion model to correlate the experimental data for single component systems. The mass transfer rate for single component systems appeared to be mainly controlled by pore diffusion. In this paper, the mass transfer coefficients for the multicomponent systems will be determined. As the solid phase concentrations of sorbent must be determined to calculate the liquid phase concentration in sorbent, an empirical method is used in the calculation of pore diffusivities for multicomponent systems. For the sorption of "metal" cations onto amorphous iron, manganese and aluminum oxides (Trivedi and Axe, 2002) the authors proposed a surface diffusion mechanism. In our paper we are using the film-pore model because the bone char is predominantly mesoporous enabling the metal ion containing solution to fill the pores and sorb onto the surface by pore diffusion.

Empirical Equation for Solid Phase Concentration

This method uses single component equations to correlate the multicomponent kinetic data. However, the sorption of cadmium and zinc ions onto bone char in multicomponent systems will experience competition from copper ions. The Langmuir-type equation cannot be used to correlate the sorption of cadmium and zinc ions in multicomponent systems except in the case of cadmium sorption in the Cd-Zn system. Therefore, an empirical Langmuir-type equation (Eq. (17)) is used in place of the Langmuir equation (Eq. (9)) to obtain better fit for the sorption of cadmium and zinc ions.

The Langmuir equation and the empirical Langmuir-type equation are separately used to correlate the experimental data. The empirical method, developed in the present research, utilizes the same equations as in the single component system except for the calculation of the solid phase concentration on the sorbent surface. The most important assumption in the film-pore diffusion model for cadmium and zinc sorption is that the solid phase concentration of sorbent at radius r can be calculated by the empirical equation. Therefore, the solid phase concentration of sorbate is assumed to be at local equilibrium at radius r. As a result, the local equilibrium of the exhausted sorbent is constant irrespective of the radius at a given time. Hence, the pore diffusivity is estimated based on the empirical equation.

Figures 5(a)–(c) show the sorption equilibrium isotherms for three metal ions in both single and multicomponent systems and the low-concentration region for the sorption of Cd, Cu and Zn ions onto Bone Char is shown in Figs. 6(a)–(c). The sorption equilibrium of copper ions in the multicomponent systems is well correlated by the Langmuir equation for all systems. In addition, the sorption of cadmium ions in the Cd-Zn solution shows a very good Langmuir fit isotherm. Therefore, the Langmuir equation will be incorporated into the film-pore diffusion model to correlate the kinetic data in these sorption systems. However, cadmium or zinc ions are competing with and being displaced by the copper ions in the multicomponent systems, and so the empirical Langmuir-type equation has been used to

Table 3. The parameters of empirical and langmuir-type equations for the sorption of cadmium, copper and zinc ions onto bone char from single and multicomponent systems.

	Cd	Cd-Cu	Cd-Zn	Cd-Cu-Zn
a_L (dm^3/mg)	1.40	0.33	0.20	0.09
q_m (mg/g)	53.7	33.6	38.9	27.5
H (mg/g)	–	0.03	–	0.019
	Cu	Cu-Cd	Cu-Zn	Cd-Cu-Zn
a_L (dm^3/mg)	1.09	0.35	0.187	0.15
q_m (mg/g)	45.0	36.2	42.0	30.2
H (mg/g)	–	–	–	–
	Zn	Zn-Cd	Zn-Cu	Zn-Cd-Cu
a_L (dm^3/mg)	0.95	0.19	0.46	0.15
q_m (dm^3/g)	33.0	22.0	20.4	13.7
H (mg/g)	–	0.02	0.04	0.03

correlate the sorption equilibria for cadmium and zinc ions. The constants for the empirical Langmuir-type and Langmuir equations are shown in Table 3.

According to Harriott equation (Tien, 1994), the interphase mass-transfer coefficient between liquid and suspended particles in an agitated vessel, k_f, and the mass-transfer coefficient of the same particles moving at their terminal velocity, u_T, through the same liquid, k_f^*, may be approximated by the relationship:

$$\frac{k_f}{k_f^*} \cong 2.0 \tag{20}$$

To estimate k_f^*, Harriott suggested using the following equation:

$$\frac{k_f^* d_p}{D_m} = 2.0 + 0.6\left[\frac{d_p u_T}{\mu}\right]^{0.5}\left[\frac{\upsilon}{D_m}\right]^{0.33} \tag{21}$$

The terminal velocity, u_T, may use the correlation of Nienow (15), given as:

$$u_T = \frac{0.153 g^{0.71} d_p^{1.14} \Delta\rho^{0.77}}{\rho^{0.29}\mu^{0.43}} \tag{22}$$

where g is the gravitational acceleration (980 cm/s^2) and $\Delta\rho = \rho_p + \varepsilon_p \rho$ is the density difference between the wet particle and the liquid density. The external mass transfer coefficients of cadmium, copper and zinc ions onto bone char using the Harriott equation are 2.46×10^{-3} cm/s, 2.44×10^{-3} cm/s and 2.41×10^{-3} cm/s, respectively.

The sorption kinetic curves for the sorption of cadmium ions in the binary and ternary systems are shown in Figs. 7(a)–(c). The concentration effect for the sorption of cadmium ions in Cd-Cu can be correlated very well but the mass effect in Cd-Cu, Cd-Zn and Cd-Cu-Zn systems showed some deviation from the experimental data points. Figures 8(a)–(c) show the sorption of copper ions from the Cd-Cu, Cu-Zn and Cd-Cu-Zn systems. The film-pore diffusion model, which incorporates the Langmuir equation, can correlate the kinetic data for copper systems. The concentration effect for sorption of zinc ions on Bone Char in Cd-Zn, Zn-Cu and Zn-Cu-Cd systems are shown in Fig. 9(a)–(c). The Film-Pore diffusion model provides a good correlation for Zn sorption on Bone Char in Cd-Zn and Cd-Cu-Zn system as show in Figs. 9(a) and (c) but the correlation for zinc systems in the Cd-Cu systems are not good as shown in Fig. 9(b). Tables 4 and 5 show the pore diffusivities and SSEs values of the multicomponent systems. The pore diffusivities of the single components are higher than the values of binary and ternary systems. The pore diffusivities in the ternary system for Cd, Cu and Zn are the lowest values except for cadmium in the Cd-Zn binary system which is approximately equal to the ternary value. These trends imply that the diffusion of the individual metal ions is inhibited by the other neighboring or competing metal ions such as the counter diffusion of Ca ions. Nevertheless, overall this model gives a good correlation of

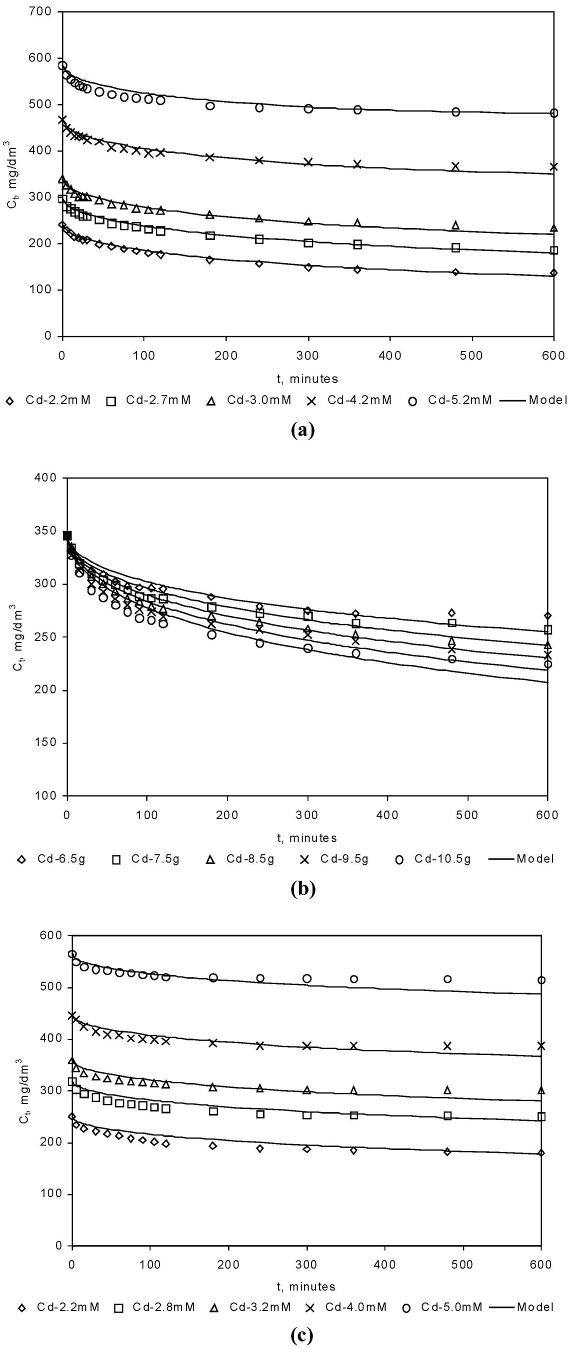

Figure 7. Concentration and mass effect for the sorption of Cd ions from Cd-Cu (a), Cd-Zn (b) and Cd-Cu-Zn (c) solutions onto bone char using the film-pore diffusion equation (Temperature = 20°C, pH = 4.9, Particle Size = 500–710 μm).

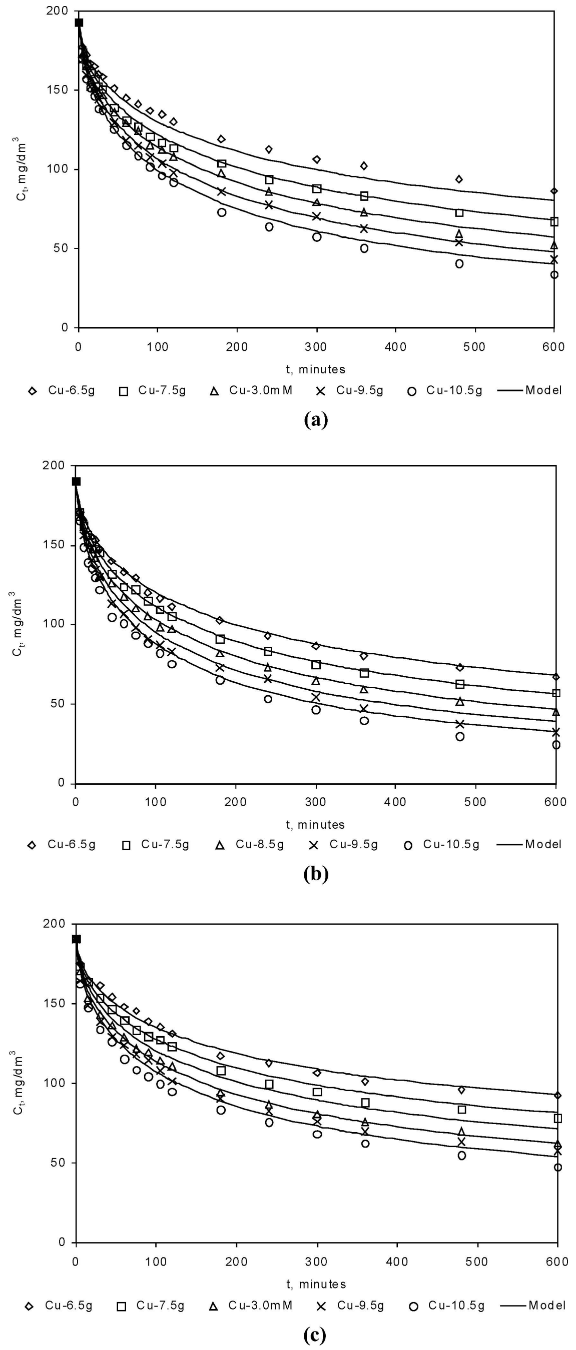

Figure 8. Mass effect for the sorption of Cu ions from Cu-Cd (a), Cu-Zn (b) and Cd-Cu-Zn (c) solutions onto bone char using the film-pore diffusion equation (Temperature = 20°C, pH = 4.9, Particle Size = 500–710 μm).

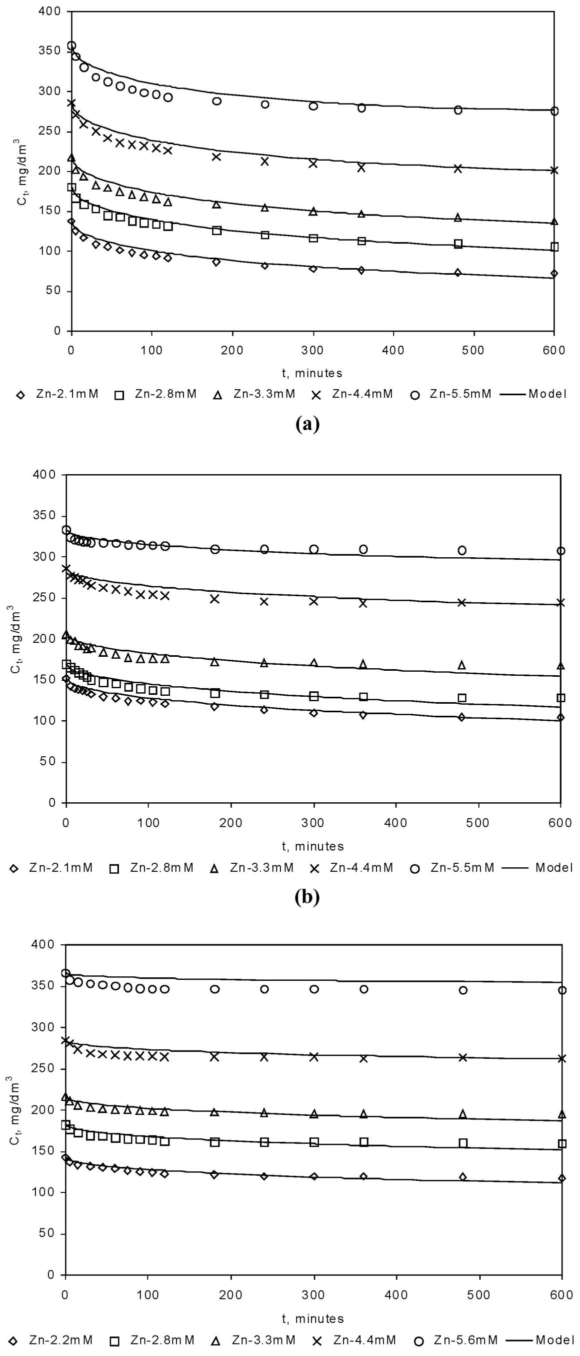

Figure 9. Concentration effect for the sorption of Zn ions from Cd-Zn (a), Cu-Zn (b) and Cd-Cu-Zn (c) solutions onto bone char using the film-pore diffusion equation (Temperature = 20°C, pH = 4.9, Particle Size = 500–710 μm).

the experimental data for three binary and one ternary systems.

The molecular diffusivities, D_m of metal ion can be calculated by the Petr Vanýsek equation (Lide and Frederikse, 1994).

$$D_m = \frac{R'T}{F^2}\left(\frac{\lambda}{|Z|}\right) \tag{23}$$

The molecular diffusivities of copper, zinc and cadmium ions are 6.47×10^{-6} cm^2/s, 6.37×10^{-6} cm^2/s and 6.52×10^{-6} cm^2/s, respectively, which are of a similar order of magnitude to the effective diffusivities. The film thickness of metal ion solution onto bone char and the tortuosity factor for sorbent can be calculated by Eqs. (24) and (25)

$$\frac{1}{S_A}N_t = -D_m\frac{dC}{dx} \cong -D_m\frac{\Delta C}{\Delta x} \rightarrow \Delta x = \frac{D_m}{k_f} \tag{24}$$

$$D_{\text{eff}} = \frac{\varepsilon_p}{\tau_f}D_m \tag{25}$$

where S_A is the external surface area of the sorbent and Δx is the thickness of the liquid film; ε_p and τ_f are intrinsic properties of sorbent, representing its porosity and tortuosity factor. The calculated film thicknesses are equivalent to 2.65×10^{-3} cm. According to Helfferich (1995), the liquid film thickness is around 10^{-3} to 10^{-2} cm for ion exchangers. Therefore, the calculated values are close to the literature values. The tortuosity factors of Cu^{2+}, Zn^{2+} and Cd^{2+} ions are shown in Table 6. The tortuosity factors of three metal ions are very close and the average tortuosity factor for these three system is equal to 2.10 ± 0.25.

Seo and Lee (1995) studied the sorption of cadmium, copper and zinc ions onto CaHAP, and determined values for the pore diffusivities of 2.95×10^{-6} cm^2/s, 2.88×10^{-6} cm^2/s and 2.77×10^{-6} cm^2/s, respectively. These values of pore diffusivities are of a similar order of magnitude to those obtained in the present studies. The discrepancy of pore diffusivities may be due to the difference of pore size distribution of the sorbent. The pore structure of bone char is the intrinsic nature of the animal bone (see Fig. 2). As the CaHAP is derived from the precipitation of CaHAP, the pore size distribution of bone char may be different to CaHAP. Therefore, the pore diffusivities obtained from Seo and Lee are different to this research.

Table 4. The pore diffusivities of multicomponent systems using the film-pore diffusion model and empirical method.

Metal ions	Single component (cm^2/sec)	Cd-Cu (cm^2/sec)	Cd-Zn (cm^2/sec)	Cu-Zn (cm^2/sec)	Cd-Cu-Zn (cm^2/sec)
Cd	1.14×10^{-6}	5.14×10^{-7}	1.98×10^{-7}	–	2.01×10^{-7}
Cu	1.39×10^{-6}	1.16×10^{-6}	–	1.39×10^{-6}	1.12×10^{-6}
Zn	1.21×10^{-6}	–	5.72×10^{-7}	2.78×10^{-7}	2.06×10^{-7}

Table 5. The SSEs (mM^2) for multicomponent systems using the film-pore diffusion model and empirical method.

Metal ions	Cd-Cu	Cd-Zn	Cu-Zn	Cu-Zn-Cd
Cd (Empirical-FP model)	1.17	1.77	–	1.57
Cu (Empirical-FP model)	0.95	–	2.10	1.61
Zn (Empirical-FP model)	–	0.90	2.06	0.93

Contribution of Surface Diffusion to the Film-Pore Diffusion Model

In the film pore diffusion process, the effective diffusivity, D_{eff}, is equal to the constant pore diffusivity, D_p. That means the metal ions diffuse along the pore and adsorb on the sorption sites. If surface diffusion takes place during adsorption, the effective diffusivity should be considered as "combined diffusion":

$$N_t = D_{\text{eff}} \frac{\partial C_{e,t}}{\partial r} = D_p \frac{\partial C_{e,t}}{\partial r} + \rho_p D_s \frac{\partial q_{e,t}}{\partial r} \quad (26)$$

The first term of Eq. (23) represents the diffusion of sorbate in the pore-liquid. The second term is equal to the surface diffusion of sorbate migration on the pore wall. Then Eq. (26) can be factorized in terms of radial concentration gradient:

$$N_t = \left(D_p + \rho_p D_s \frac{\partial q_{e,t}}{\partial C_{e,t}} \right) \frac{\partial C_{e,t}}{\partial r} \quad (27)$$

and D_{eff} can be represented by

$$D_{\text{eff}} = D_p + \rho_p D_s \frac{\partial q_{e,t}}{\partial C_{e,t}} \quad (28)$$

In the studies of surface diffusion, Darken (1948) proposed the surface diffusion in terms of chemical potential, which results in Eq. (29):

$$D_s = D_{s,o} \left(\frac{d \ln C_{e,t}}{d \ln q_{e,t}} \right) \quad (29)$$

The Langmuir isotherm can be used to simplify the term $\frac{\partial q_{e,t}}{\partial C_{e,t}}$ in Eq. (27) because this term is equal to the slope of the adsorption isotherm, therefore, the effective diffusion can be represented:

$$D_{\text{eff}} = D_p + \frac{q_m a_L \rho_p D_{s,o}}{(1 + a_L C_{e,t})} \quad (30)$$

Equation (30) is substituted into the film-pore diffusion model to generate the film-pore surface diffusion model. The results are shown in Table 7. Comparing the SSEs of the three sorption systems, the film-pore surface model using in the sorption of copper and zinc ions can slightly improve the fitting of the experimental data. The difference of SSEs between the film-pore and the film-pore-surface diffusion model for the copper and zinc systems are around four percent while the improvement for the sorption of cadmium ions is around two percent. The contribution of the surface diffusion to the intraparticle mass transfer is less than 2% in three metal ions systems. This proved that the pore diffusion was the main rate-controlling mechanism in

Table 6. The values of molecular diffusivity, film thickness and tortuosity factor for three metal ions.

	Cu^{2+}	Zn^{2+}	Cd^{2+}
Molecular diffusivities of ion in solutions (cm^2/s)	6.47×10^{-6}	6.37×10^{-6}	6.52×10^{-6}
Calculated film thickness (cm)	2.65×10^{-3}	2.65×10^{-3}	2.65×10^{-3}
Tortuosity factor	1.91	2.17	2.34

Table 7. The pore diffusivities, surface diffusivities and SSE for the film-pore surface diffusion model at 3 mM.

	Cu^{2+}	Zn^{2+}	Cd^{2+}
D_p (cm^2/s)	1.39×10^{-6}	1.20×10^{-6}	1.14×10^{-6}
$D_{s,o}$ (cm^2/s)	2.4×10^{-8}	2.7×10^{-8}	1.0×10^{-8}
D_{eff} (cm^2/s)			
Film-pore	1.39×10^{-6}	1.21×10^{-6}	1.14×10^{-6}
	↓	↓	↓
Film-pore surface	1.41×10^{-6}	1.22×10^{-6}	1.16×10^{-6}
SSE			
Film-pore	2.15	1.28	1.03
	↓	↓	↓
Film-pore surface	2.09	1.23	1.00

the sorption of copper, zinc and cadmium onto bone char.

Nomenclature

a_L	Langmuir isotherm constant (dm^3/mg)
C_o	Initial liquid-phase concentration (mg/dm^3)
C_e	Equilibrium liquid-phase concentration (mg/dm^3)
$C_{e,t}$	Tie line liquid-phase concentration at particle surface at time t (mg/dm^3)
C_t	Liquid-phase concentration at time t (mg/dm^3)
$(C_t)_{\text{exp}}$	Experimental values of liquid-phase concentration at time t (mg/dm^3)
$(C_t)_{\text{cal}}$	Calculated values of liquid phase concentration at time t (mg/dm^3)
d_p	Diameter of sorbent (cm)
D_{eff}	Effective diffusivity (cm^2/s)
D_m	Molecular diffusivity (cm^2/s)
D_p	Pore diffusivity (cm^2/s)
$D_{s,o}$	Corrected surface diffusivity (cm^2/s)
D_s	Surface diffusivity (cm^2/s)
F	Faraday constant
H	Henry constant (mg/g)
k_f	External mass transfer coefficient (cm/s)
K_L	Langmuir isotherm constant (dm^3/g)
n	Number of experiments
N_t	Mass transfer rate (mg/s)
q_e	Equilibrium solid-phase concentration (mg/g)
$q_{e,t}$	Tie line solid-phase concentration at time t (mg/g)
$q_{e,h}$	Hypothetical equilibrium concentration on sorbent surface. (mg/g)
q_m	Monolayer capacity of Langmuir equation (mg/g)
q_t	Mean equilibrium solid-phase concentration at time t (mg/g)
r	Radius of concentration front of metal ions penetrating adsorbent (cm)
R	Radius of adsorbent particle (cm)
R'	Gas constant (J/mol K)
R_m	Constant in quadratic Eq. (18), $R_m = (1 - (r/R)^3)(W/V)$ (mg/dm^3)
S_A	Surface area of sorbent (m^2/g)
t	Contact time hrs
u_T	Liquid-phase volume (dm^3)
V	Liquid-phase volume (dm^3)
Δx	Film thickness (cm)
W	Weight of sorbent (g)
Z	The charge on the ion
ψ	Relationship between film and intraparticle diffusion, $\psi = 1 + D_{\text{eff}} r/(k_f R(R - r))$
λ	Ionic conductivity of ion (m^2s/mol)
ε_p	Porosity
τ_f	Tortuosity factor
ρ	Particle density (g/dm^3)
μ	Viscosity of solvent (cp)
ν	Kinematic Viscosity (cp)

References

Abdel Raouf, M.W. and A.A.M. Daifullah, "Potential Use of Bone Charcoal in the Removal of Antimony and Europium Radioisotopes from Radioactive Wastes," *Ads. Sci. Technol.*, **15**(7), 559–569 (1997).

Bennett, M.C. and J.C. Abram, "Adsorption from Solution on the Carbon and Hydroxyapatite Components of Bone Char," *J. Coll. Interf. Sci.*, **23**, 513–521 (1967).

Bhargava, D.S. and D.J. Killedar, "Batch Studies of Water Defluoridation using Fishbone Charcoal," *Research J. Water Pollut. Control Federal*, **63**, 848–858 (1991).

Cheung, C.W., C.K. Chan, J.F. Porter, and G. McKay, "Combined Diffusion Model for the Sorption of Cadmium, Copper and Zinc Ions onto Bone Char," *Environ. Sci. Technol.*, **35**, 1511–1522 (2001).

Cheung, C.W., C.K. Chan, J.F. Porter, and G. McKay, "Film-Pore Diffusion Control for the Batch Sorption of Cadmium Ions from Effluents onto Bone Char,"*J. Coll. Interf. Sci.*, **234**, 328–336 (2001).

Christoffersen, J., M.R. Christoffersen, R. Larsen, and I.J. Moller, "Regeneration by Surface-Coating of Bone Char Used for Defluoridation of Water," *Water Research*, **25**, 227–229 (1991).

Do, D.D. *Adsorption Analysis: Equilibria and Kinetics*, Singapore, Imperial College Press, 1998.

Elliott, J.C., *Studies in Inorganic Chemistry 18, Structure and Chemistry of the Apatites and other Calcium Orthophosphates*, Chapter 3, pp. 111–189, Elsevier Press, New York, 1994.

Furusawa, T. and J.M. Smith, "Fluid-Particle and Intraparticle Mass Transport Rates in Slurries," *Ind. Eng. Chem. Fundam.*, **12**, 197–203 (1973).

Girgis, B.S., A. Abdel Kader, and A.N.H. Aly, "Development of Porosity in Bone Char during Decolourization of Sugar Syrup," *Ads. Sci. Technol.*, **15**, 277–287 (1997).

Gu, B., L. Liang, M.J. Dickey, X. Yin, and S. Dai, "Reductive Precipitation of Uranium (VI) by Zero-valent Iron," *Environ. Sci. Techno.*, **32**, 3366–3373 (1998).

Hatsushika, T., H. Sakane, and T. Suzuki, "Cation Exchange Characteristics of Modified Synthetic Hydroxyapatites and Calcium Carbonates," *The Proceedings of the Fifth International Conference on Ion Exchange Processes*, pp. 187–190, Advances in Ion Exchange for Industry and Research, The Royal Society of Chemistry, Cambridge, 1999.

Larsen, M.J., E.I.F. Pearce, and S.J. Jensen, "Defluoridation of Water at High pH with Use of Brushite, Calcium Hydroxide, and Bone Char," *J. Dental Research*, **72**, 1519–1525 (1993).

Lewis, J., "The Use of Bone Charcoal in the Treatment of Rural Water Supplies," *J. Ch. Instn. Wat. Envir. Mangt.*, **9**, 385–395 (1995).

Lide, D.R. and H.P.R. Frederikse, *CRC Handbook of Chemistry and Physics*, 74th ed., CRC Press, London, 1994.

Phantumvanit, P. and R.Z. LeGeros, "Characteristics of Bone Char Related to Efficacy of Fluoride Removal form Highly Fluoridated Water," *Fluoride*, **30**, 207–218 (1997).

Seo, Y.G. and D. Lee, "Removal of Heavy-metal Ions from Aqueous Solution by Hydroxyapatite," *Hwahak Konghak*, **33**, 360–366 (1995).

Suzuki, T., T. Hatsushika, and M. Miyake, "Removal of Toxic Ions by Apatites as a Lattice on Ion-exchanger," in *International Conference on Ion Exchange*, pp. 401–406, Japan, Tokyo, 1991.

Suzuki, T., T. Hatsushika, and M. Miyake, "Synthetic Hydroxyapatites as Inorganic Cation Exchangers," *J. Chem. Society-Faraday Trans. I*, **78**, 3605–3611 (1982).

Suzuki, T., K. Ishigaki, and N. Ayuzawa, "Removal of Toxic Pb^{2+} Synthetic Hydroxyapatites," *Chem. Eng. Commun.*, **34**, 143–151 (1985).

Tien, C., *Adsorption Calculations and Modeling*, 1st edn., Butterworth-Heinemann, Boston.

Trivedi, P. and L. Axe, "Modeling Cd and Zn Sorption to Hydrous Metal Oxides," *Environ. Sci. & Technol.*, **34**, 2215–2223 (2000).